

Analysis of four different models for quantifying tomato transpiration in a soilless greenhouse

Msc. Thesis by Koen Harms

Supervisors: Dr. ir. M. ten Veldhuis,
Dr. ir. A.M.J. Coenders,
Ir. A. van Klink

3rd Corrector: Prof.Dr.ir. R. Uijlenhoet

Water Resources Group
16-06-2022

Student number: 4392558

Analysis of four different models for quantifying tomato transpiration in a soilless greenhouse

Master thesis Water Resources Management submitted in partial fulfilment of the Master of Science degree Water Management at Technical University Delft, The Netherlands

Koen Harms

June 2022

Supervisor (chair):

Dr. ir. M. ten Veldhuis

Water Resources Group

Delft University of Technology

The Netherlands

<https://www.tudelft.nl/en/ceg/about-faculty/departments/watermanagement>

Internship Company

Delphy Improvement Centre B.V., Violierenweg 3, 2665 MV Bleiswijk, The Netherlands

Abstract

Calculations to predict the irrigation water demands in commercial vegetable greenhouses are often based on outside solar radiation measurements and drainage volumes. Although these calculations are relatively simple to implement, this system does not always result in optimal irrigation water delivery. Furthermore, it needs constant monitoring and adjustment by the grower. Scientific literature points to several models used to calculate the transpiration of vegetable crops inside a greenhouse but the results are hard to compare since different experiment setups were used. This study aimed to analyse the accuracy of four different transpiration models, Penman-Monteith, Stanghellini, Priestley-Taylor, and Takakura for the calculation of tomato transpiration inside a soilless greenhouse. By addressing this knowledge gap the outcome of this study provides a step towards more autonomy in vegetable horticulture. During the summer a three month experiment was conducted in a Venlo-type soilless greenhouse in The Netherlands. The air temperature, relative humidity, wind speed and net radiation were measured inside a tomato greenhouse. Hourly transpiration data measured using a combination of sap flow sensors and lysimeters, was compared to the four different models. The Penman-Monteith and Priestley-Taylor models, intended for outdoor use, had a similar accuracy as the Stanghellini and Takakura models that are developed for Venlo-type soilless greenhouse. When comparing the models error range to the average hourly transpiration, it is found that the models are not accurate enough for irrigation scheduling. A model sensitivity analysis illustrates how changes in net radiation, temperature, humidity and wind speed affect modelled tomato transpiration. A recommendation on methods to improve model accuracy is made.

Table of Content

Abstract	II
1 Introduction.....	1
1.1 Relevance: Understanding the Greenhouse Water Cycle	1
1.2 Problem statement: Calibration of Greenhouse Transpiration Models	2
1.3 Research objective	2
1.4 Research question	2
2 Theoretical framework: Transpiration of a Greenhouse Crop Based on Microclimate Conditions.....	3
2.1 Penman-Monteith	4
2.2 Stanghellini	6
2.3 Priestley-Taylor.....	7
2.4 Takakura	7
3 Materials and Method.....	8
3.1 Approach	8
3.2 Greenhouse Description.....	8
3.3 Measuring Equipment Greenhouse Meteorological Data	9
3.4 Tomato Crop Transpiration Measurement	10
3.5 Data Filtering	11
3.6 Methods Used to Determine Model Accuracy.....	11
4 Results	13
4.1 Evaluation of Aerodynamic and Internal Resistances	13
4.2 Accuracy of the Transpiration Modelling	15
4.2.1 Time Series	15
4.2.2 Scatterplot Modelled vs Measured	18
4.2.3 Error Density Distribution.....	19
4.2.4 Cumulative Transpiration	20
4.3 Individual Parameter Sensitivity of the Transpiration Models.....	21
4.3.1 10% Change Table	22
4.3.2 Scenario Distribution	23
5 Discussion	25
6 Conclusions.....	27
References.....	29
Annex A: Abbreviations	31
Annex B: Pictures Inside Greenhouse	32

1 Introduction

1.1 Relevance: Understanding the Greenhouse Water Cycle

Greenhouse cultivation protects crops from adverse weather conditions and predators while allowing year-round production and improved control over pests and diseases. A further benefit is the ability to cultivate crops on latitudes that have climate conditions that are not suitable for plant growth. These benefits incentivized a global increase in greenhouse cultivated area, towards an estimated 405000 ha of greenhouses throughout Europe (Rakhmanin & Dreyer, 2017). The Dutch sector constitutes 4989 ha of Venlo-type greenhouses of which 1846 ha tomatoes (CBS, 2022). These greenhouses fall into the category 'high technology', as the climate is controlled by a computer, and the construction is made of galvanized iron support structures, aluminium glass supports, and a glass cover. This horticulture sector's production accounts for 45.5% of the total intra-EU export of tomatoes in a 7.3 billion Euro market (Eurostat, 2019). Since tomatoes are in The Netherlands the largest crop in both acreage and revenue it is decided to study tomato transpiration.

Tomato crops grown in a greenhouse are shielded from rainfall and thus require adequate irrigation at the right time in order to minimize water stress and maximize yield. Excess water may harm the crops by causing waterlogging and root damage, while insufficient irrigation leads to weaker plants and poor crop yield (Acquah, et al., 2018). To maintain root tissue permeability roots require an oxygen supply from the atmosphere, transported to the roots by the pore system of the growing medium. Since the diffusion coefficient of oxygen in water is a multitude of times larger than in air, a growing medium filled with water will prevent oxygen from reaching the roots. If the water supply is insufficient plants will lose their rigidity and wilt. In the plant water is an essential transport medium for salts and assimilates, and furthermore the facilitator of chemical reactions in assimilation and respiration (Moene & van Dam, 2014). Typical water content of tomato fruits is larger than 95%. This makes the availability of water, in sufficient quantity, essential for a high quality, and thus high-valued, final product.

The greenhouse cover makes it possible to regulate the temperature and humidity by means of heating pipes and ventilation windows. In Venlo-type greenhouses the adoption of soilless systems made transpiration the largest component of the greenhouse water cycle, since water is no longer leaching into the soil. Largely decoupled from the outside atmosphere, a unique microclimate is formed by the accumulation of heat and water released at the crop surface. Consequently, the transpiration rate of greenhouse crops will reach a stable equilibrium transpiration rate, dependent on the net radiation received and the permeability of the cover for water vapour (Katsoulas et al., 2019). The resistance to water vapour transport in greenhouses can become much higher than that of an open field due to low windspeeds and turbulence. As a consequence, the crop is not only strongly decoupled from the outside atmosphere, but also from the greenhouse atmosphere (Katsoulas et al., 2019).

Estimations on the transpiration of a greenhouse crop are largely dependent of greenhouse characteristics and the ability to control relevant greenhouse climate factors (Katsoulas et al., 2019). Greenhouse characteristics include variables such as shape, dimensions, cover material, and orientation in relation to the sun. Additionally, growers can grow crops in the natural soil or choose for a soilless system with various different growing media. Greenhouse climate factors are temperature, relative humidity, radiation, ventilation, heating, artificial lighting and shading. Reliable models for plant water transpiration must take these factors into account and provide a method to link greenhouse climate to tomato transpiration.

1.2 Problem statement: Calibration of Greenhouse Transpiration Models

Traditionally, irrigation management in commercial vegetable production has been based on the accumulated experience of growers and technical advisors (Thompson et al., 2020). In Venlo-type greenhouse cultivation, however, the indoor climate is both monitored and controlled by a climate computer. Currently, the irrigation water demand is predicted based on the outside solar radiation, in combination with an adjustment using drainage volumes. Researchers at the Delphy Improvement Centre have observed that this system does not always result in optimal irrigation water delivery. The most critical period is spring, when sudden increases in radiation and temperature lead to insufficient water delivery and rapid adjustments by the growers (Internal communication Delphy, 2021). It is uncertain how climate variables, such as temperature, humidity, and turbulence in the air, can be incorporated in greenhouse transpiration models.

Current technology to monitor greenhouse crop water fluxes are weighing lysimeters, sap flow measurements and stem diameter gauges. The problem with these methods is that they are difficult to implement in cultivation practices, as they are retrospective. The sensors monitor what has happened in the greenhouse, while growers are in need of methods to proactively adjust greenhouse conditions and irrigation to the climate conditions in the near future. Modelling of crop transpiration is seen as an alternative method to quantify crop water use (Villarreal-Guerrero, et al., 2012); (Katsoulas & Stanghellini, 2019). Accurately measuring and modelling transpiration is critical for optimizing greenhouse water management. Finding and analysing reliable descriptive models is the first step towards the ultimate goal of a forecasting model.

Knowledge of crop transpiration at relatively short time intervals (hours) is necessary for precise management of irrigation water and greenhouse climate. Scientific literature points to several different models to indirectly calculate transpiration in greenhouses (Karacaet al., 2018; Katsoulas & Stanghellini, 2019). This study includes the Penman-Monteith, Priestley-Taylor, Stanghellini, and Takakura models. An explanation of the different models and their assumptions can be found in Section 2, which describes the Theoretical Framework. Each greenhouse type has a different microclimate and climate control equipment (shading, artificial lighting, humidification, heating and ventilation) affecting the physical transpiration process. Therefore, results from different studies on transpiration model performance is difficult to compare. These existing models have to be analysed in a single experiment to know whether they can produce reliable and accurate results for transpiration of tomato plants in greenhouse cultivation.

1.3 Research objective

The objective for this research is to provide a recommendation on the most accurate model for the calculation of the irrigation water demand of tomato plants grown in a Venlo-type soilless greenhouse. This is done by comparing four different transpiration models (Penman-Monteith, Priestley-Taylor, Stanghellini, and Takakura) that establish transpiration rates in greenhouse cultivation. The model validity is checked by comparison with measurements of transpiration by weighing lysimeters combined with sap-flow sensors. When the water demand can be met more exactly, this will ensure the plants do not experience water stress during their growth and thus production security is improved. Finally, this study aims to identify the most dominant parameters for predicting transpiration rates of tomato plants grown in a greenhouse.

1.4 Research question

To address the existing knowledge gap, this research will answer the following research question:

How accurately can tomato transpiration in a greenhouse be reproduced in relation to the number of observed variables in the reproduction model?

To aid answering this research question the following sub-questions are defined:

1. How accurately can existing models reproduce tomato transpiration observations in a Venlo-type soilless greenhouse?
2. What is the sensitivity of the individual parameters in the different transpiration models?
3. Which parameters constitute the best performing transpiration model?

2 Theoretical framework: Transpiration of a Greenhouse Crop Based on Microclimate Conditions

Transpiration is defined as the change of state of water from liquid to vapor that occurs in the stomatal cavities of leaves (Miralles et al., 2020). Water is absorbed by the roots from the growing media and transported as a liquid to the leaves via xylem. In the leaves water is allowed to escape as vapor by small pores, called stomata. These stomata regulate the rate of transpiration by opening and closing. This process of transpiration keeps the cells turgid, helps the transport of minerals from the rootzone to different parts of the plant, and regulates the temperature of the leaves (Moene & van Dam, 2014).

Crop transpiration can be determined with indirect climate-based models, or with direct measurement by weighing lysimeters or drainage balances (Incrocci, et al., 2020). Weighing lysimeters that directly measure the loss of water from the soil due to evaporation and from plants by transpiration, are the most accurate measurement of transpiration (Acquah, et al., 2018). The indirect climate-based models as described in this study estimate the transpiration based on meteorological conditions (e.g., temperature, humidity, wind speed, radiation) and plant characteristics like leaf area index (LAI) and resistance to water vapour transport. In this study soil moisture is neglected as the tomato plants are grown in rockwool slabs covered in impermeable plastic.

Based on a literature study four models are chosen to be analysed in an experimental greenhouse: Penman-Monteith, Stanghellini, Priestley-Taylor, and Takakura (Equation 1-4). The Penman-Monteith and Stanghellini models are physically based, whereas the models Priestley-Taylor and Takakura are empirically derived simplifications of Penman-Monteith. The Stanghellini and Takakura models are specially developed for the use in greenhouses (Stanghellini, 1987; Takakura et al., 2009), while the Penman-Monteith and Priestley-Taylor models were developed for outdoor use (Allen et al., 1998; Priestley & Taylor, 1972). These four models are chosen because they are used to estimate transpiration inside greenhouses in different studies (Donatelli et al., 2006; Gong et al., 2020; Incrocci et al., 2020; Karaca et al., 2018; Katsoulas & Stanghellini, 2019). In the following sections the four models will be explained (Section 2.1-2.4).

$$\text{Penman - Monteith: } LE = \frac{\Delta(R_n - G) + \rho_a c_p \frac{(e_s - e_a)}{r_a}}{\Delta + \gamma \left(1 + \frac{r_s}{r_a}\right)} \quad \text{With } r_a = r_a^p \quad (1)$$

$$\text{Stanghellini: } LE = \frac{\Delta(R_n - G) + \left(\rho_a c_p \frac{2 LAI(e_s - e_a)}{r_r}\right)}{\Delta + \gamma \left(1 + \frac{r_i}{r_a}\right)} \quad \text{With } r_a = r_a^s \quad (2)$$

$$\text{Priestley - Taylor: } LE = \alpha \frac{\Delta}{\Delta + \gamma} R_n - G \quad (3)$$

$$\text{Takakura: } LE = R_n - h(T - T_w) - G \quad (4)$$

Table 1, Explanation of symbols used in (Equations 1 – 4)

Model	Explanation of symbols	Reference
Penman-Monteith	LE Reference evaporation [W m^{-2}] Δ Slope vapour pressure curve [$\text{Pa } ^\circ\text{C}^{-1}$] R_n Net radiation at the crop surface [W m^{-2}] G Soil heat flux density [W m^{-2}] ρ_a Mean atmospheric density at constant pressure [kg m^{-3}] C_p Specific heat of air [$\text{J kg}^{-1} ^\circ\text{C}^{-1}$] e_a Actual vapour pressure [Pa] e_s Saturation vapour pressure [Pa] γ Psychrometric constant [$\text{Pa } ^\circ\text{C}^{-1}$] r_a^p Aerodynamic resistance [s m^{-1}] r_s Surface resistance [s m^{-1}]	(Allen et al., 1998)
Stanghellini	LAI Leaf area index [$\text{m}^2 \text{m}^{-2}$] r_a^s Aerodynamic resistance [s m^{-1}] r_r Radiative resistance [s m^{-1}] r_i Internal resistance [s m^{-1}]	(Stanghellini, 1987)
Priestley-Taylor	α Dimensionless constant (1.26)	(Priestley & Taylor, 1972)
Takakura	h Coefficient of the convective heat transfer [$\text{W m}^{-2} ^\circ\text{C}^{-1}$] T Air temperature [$^\circ\text{C}$] T_w Leaf surface temperature [$^\circ\text{C}$]	(Takakura, et al., 2009)

2.1 Penman-Monteith

The Penman-Monteith model, Equation 1 is an extended version of the original Penman equation for transpiration from wet surfaces. To make the link from transpiration from a wet surface to transpiration by vegetation the concept of the ‘big leaf’ is introduced. All vegetation is simplified to one single leaf, the ‘big leaf’, which is given one idealized stomatal cavity (Figure 1). All water vapour is assumed to originate from the plants stomata, and thus the method aims to describe the process of transpiration. Because of these assumptions the method is limited to surfaces that are fully covered by vegetation. A mixture of plants and bare soil cannot be described as this would introduce new pathways for water vapour to evaporate (Moene, & Van Dam, 2014).

In literature the Penman-Monteith model is often divided in an aerodynamic and radiation term by splitting the equation terms into two. The left numerator ($\Delta(R_n - G)$) in the equation describing the radiation, and the right numerator ($\rho_a c_p \frac{(e_s - e_a)}{r_a}$) the aerodynamic processes of transpiration (Allen et al., 1998). The Penman-Monteith standardized method supports both daily and hourly calculation time steps for transpiration (Pereira et al., 2015).

When a plant transpires, water vapour does not originate from the leaf surface but from within the stomatal cavity. The air within the stomatal cavity is assumed to be permanently saturated with water vapour, at the surface temperature of the leaf. The transport from within the leaf to the surface experiences a separate resistance, the surface resistance r_s . This resistance acts in series with the aerodynamic resistance r_a (Moene, & Van Dam, 2014).

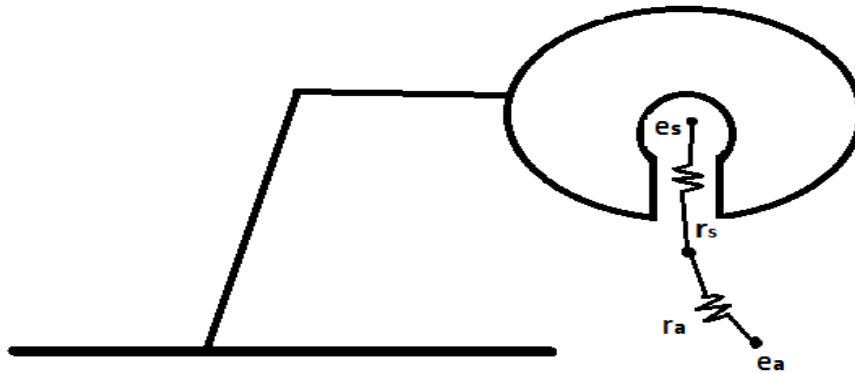


Figure 1, The 'big leaf' simplification: one stomatal cavity for the complete canopy. Water vapour transport experiences two resistances in series; r_s (surface resistance) and r_a (aerodynamic resistance). The air within the stomatal cavity is permanently saturated (e_s). The saturation of the ambient air (e_a) depends on the temperature. Adapted from: Moene & Van Dam (2014).

This surface resistance is the main determining factor for the partitioning of available energy between latent heat flux and sensible heat flux. When the surface resistance is large, transpiration will be reduced, whereas for small values of the surface resistance most available energy is used for transpiration (Moene & van Dam, 2014).

The Penman-Monteith equation calculates the potential evapotranspiration rate from a reference crop canopy. The computation of the parameters used in the equation is standardized, making the Penman-Monteith method an internationally accepted standard method for reference transpiration (Pereira et al., 2015). The Penman-Monteith method has been used in various studies, and included into several computer programs and software used for irrigation scheduling (Pereira et al., 2015; Zotarelli et al., 2020). This is because of its acceptable accuracy and relative simplicity (Incrocci et al., 2020).

The application of the Penman-Monteith model requires knowledge on microclimate variables that are not easily available. The aerodynamic resistance (r_a^p) depends on the air velocity around and within the crop canopy. In the original Penman-Monteith equation aerodynamic resistance is a function of wind speed, however this will approach infinite when windspeeds are close to zero, which is the norm inside a greenhouse (Allen et al., 1998). Therefore it was chosen to calculate aerodynamic resistance using Equation 5 based on (De Bruin & Stricker, 2000). The surface resistance (r_s) is dependent on the opening and closing of stomata and can be described as the resistance of vapour flow through the transpiring crop. In this study the surface resistance is calculated using, Equation 6 based on (Allen et al., 1998).

$$r_a^p = \frac{245}{(0.54 * u) + 0.5} \quad (5)$$

With: r_a^p Aerodynamic resistance [sm^{-1}]

u Wind speed [ms^{-1}]

$$r_s = \frac{r_l}{0.5 * LAI} \quad (6)$$

With: r_s Surface resistance [sm^{-1}]
 r_l Stomatal resistance [sm^{-1}]
 LAI Leaf area index [-]

The stomatal resistance (r_l) is crop specific and is influenced by the surrounding climate and the water availability. In this study the stomatal resistance is constant at 200 [sm^{-1}], which is for a well-watered tomato crop during the day (Stanghellini et al., 2019).

2.2 Stanghellini

Stanghellini revised the Penman-Monteith equation to represent greenhouse conditions, where air velocities are typically low ($< 1.0 \text{ ms}^{-1}$). The model is developed assuming a multi-layer canopy of well-developed tomato crop grown in a single glass greenhouse with hot-water pipe heating. The first difference is that the leaf area index (LAI) is used to account for energy exchange between multiple layers of leaves as present in tall greenhouse crops (Donatelli et al., 2006). The second difference is a change in the method to calculate the resistance to water vapour transport. The Stanghellini model introduced a more elaborate model where the resistance to water vapour transport depends on solar radiation (Stanghellini, 1987). The reasoning behind this change is that plants are actively opening and closing their stomata and thus in control of the water vapour exchange with their environment. Tomatoes, like most vegetables, use C3 photosynthesis to absorb sunlight and carbon dioxide to form a three-carbon compound before converting this compound into sugar. This process takes place during the day when the sun is out. At night, when the net radiation is zero or negative, the plants close their stomata to avoid excess water loss. The aerodynamic and surface resistances are calculated with a different formula, Equation 7 and 8 respectively, and the radiative resistance is introduced (Donatelli et al., 2006).

$$r_a^s = \frac{245}{(0.54 * u) + 1} \quad (7)$$

With: r_a^s Aerodynamic resistance [sm^{-1}]
 u Wind speed [ms^{-1}]

In the Stanghellini model the surface resistance is called internal resistance (r_i). In an attempt to avoid confusion this paper does the same. The internal resistance is the resistance of the leaf to the transfer of water vapour, and is influenced by the climate and water availability. Generally stomatal resistance is high during the night and low during the day when solar radiation results in the stomata opening for the plants photosynthesis (Acquah et al., 2018). This resistance is crop specific and calculated using Equation 8, based on (Stanghellini, 1987; Acquah, et al., 2018).

$$r_i = r_l * \left(1 + \frac{1}{\exp(0.05 * (R_n - 50))}\right) \quad (8)$$

With: r_i Internal resistance [sm^{-1}]
 r_l Stomatal resistance [sm^{-1}] R_n Net radiation [Wm^2]

However, there is a second condition that causes plants to decide to actively close their stomata. This happens when conditions for growth are not ideal during the day. There is a limit to the speed plants are able to take up and transport water from the roots to the leaves. When the leaf temperature

becomes too high, this leads to an imbalance in the water transport where more water vapour is lost at the leaf surface than can be supplied. During these conditions plants will close their stomata to preserve water and avoid drying out. The radiative resistance takes this process into account and is calculated using Equation 9, based on (Donatelli et al., 2006; Acquah, et al., 2018).

$$r_r = \frac{\rho_a C_p}{4 * \sigma * (T + 237.15)^3} \quad (9)$$

With:	r_r	Radiative resistance [sm^{-1}]
	ρ_a	Mean atmospheric density at constant pressure [kg m^{-3}]
	C_p	Specific heat of air [$\text{J kg}^{-1} \text{K}^{-1}$]
	σ	Stefan Boltzmann constant [$\text{J m}^{-2} \text{K}^{-4} \text{s}^{-1}$]
	T	Air temperature [$^{\circ}\text{C}$]

2.3 Priestley-Taylor

Priestley and Taylor used observations from well-watered surfaces such as water or low vegetation to find a coefficient that relates the aerodynamic term from the Penman-Monteith equation to the radiation term (Moene & van Dam, 2014). Using this coefficient simplifies the equation for transpiration to Equation 3. The hypotheses by (Priestley & Taylor, 1972) is that an air volume moving above a vegetated area with an abundant supply of water will become fully saturated with water. In these conditions the saturated and actual vapour pressure will be equal and can therefore be left out.

The Priestley-Taylor model has been used to model tomato transpiration in a plastic greenhouse with open soil, where the performance of daily transpiration calculation was found to be good with similar accuracy to the Penman-Monteith model and pan evaporation measurements (Gong et al., 2020). The Priestley-Taylor model can be used for the calculation of daily transpiration for conditions where weather input for the aerodynamic term (relative humidity and windspeed) are unavailable (Donatelli et al., 2006). In this study the dimensionless coefficient is 1.26, which is recommended by (Priestley & Taylor, 1972) for crops with an abundant water supply.

2.4 Takakura

A second simplification of the Penman-Monteith equation was proposed by (Takakura, et al., 2009). This Takakura model is based on the same heat balance method. The hypothesis of this model is that the ratio between transpiration and radiation is almost constant once a stable leaf area index (LAI) has been reached. Transpiration can then be empirically estimated from solar radiation (Incrocci, et al., 2020). The heat transfer coefficient (h) in Equation 4 is the sensible heat transfer term. According to (Takakura, et al., 2009) this coefficient is a function of wind speed when outdoors, but inside a greenhouse with vegetable crops, it was approximated by a constant of 7 [$\text{W m}^{-2} \text{ }^{\circ}\text{C}^{-1}$].

3 Materials and Method

3.1 Approach

To answer the research question two physically based models and two empirically derived models are analysed and compared, as introduced in the theoretical framework. For each model transpiration is calculated on an hourly timestep using climatic data recorded on site during this experiment. Data used in this study is collected from 2021-06-18 until 2021-09-14, and has a resolution of 5 minutes. Validation of the models is done with measured values from weighing lysimeters and high-resolution sap flow measurements in the same 5 minute time intervals.

3.2 Greenhouse Description

The data used in this study, is gathered in greenhouse 3.5 from the Delphy Improvement Centre in Bleiswijk, The Netherlands. This is a rectangular Venlo-type greenhouse with an area of 14 [m] long times 9.6 [m] wide, and a height of 4.8 [m] (Figure 2). The longer side has an South-west to North-east direction, which is the prevailing wind direction. The high tech soilless greenhouse has a hot-water steel pipe heating system, drip irrigation, and lighting. Hot and moist exhaust air from the inside of the greenhouse exchanges with the outside atmosphere via natural ventilation. In this greenhouse six rows of 30 individual tomato plants are monitored using sensors (Table 2).

This work investigates the transpiration of tomato (*Solanum Lycopersicum* L. cv. *Merlice*) plants, which is one of the main cultivars in the country. The planting medium is rockwool with mean bulk density of 50 [kg m⁻³] in the form of a slab with dimensions, 1200 [mm] long, 200 [mm] wide, and 75 [mm] height. On top of each slab grow 3 evenly spaced plants with each their own 100 [mm²] rockwool cube, that is used since seedlings. Drip irrigation is provided by a tube directly in the rootzone, where all plants receive the same fertilizer solution. The plants are given the same agronomic management practices constituting of pruning, fruit harvesting, pest control, and branch support. At the start of the experiment the plants are 8 months old, ranking them in the mid-season stage of the FAO-56 growth stages (Allen et al., 1998). During the experiment the leaf area index was 3 [m²m⁻²], which is a common value for mature tomato crops (Acquah, et al., 2018).

For pictures of the inside of the greenhouse see Annex B.

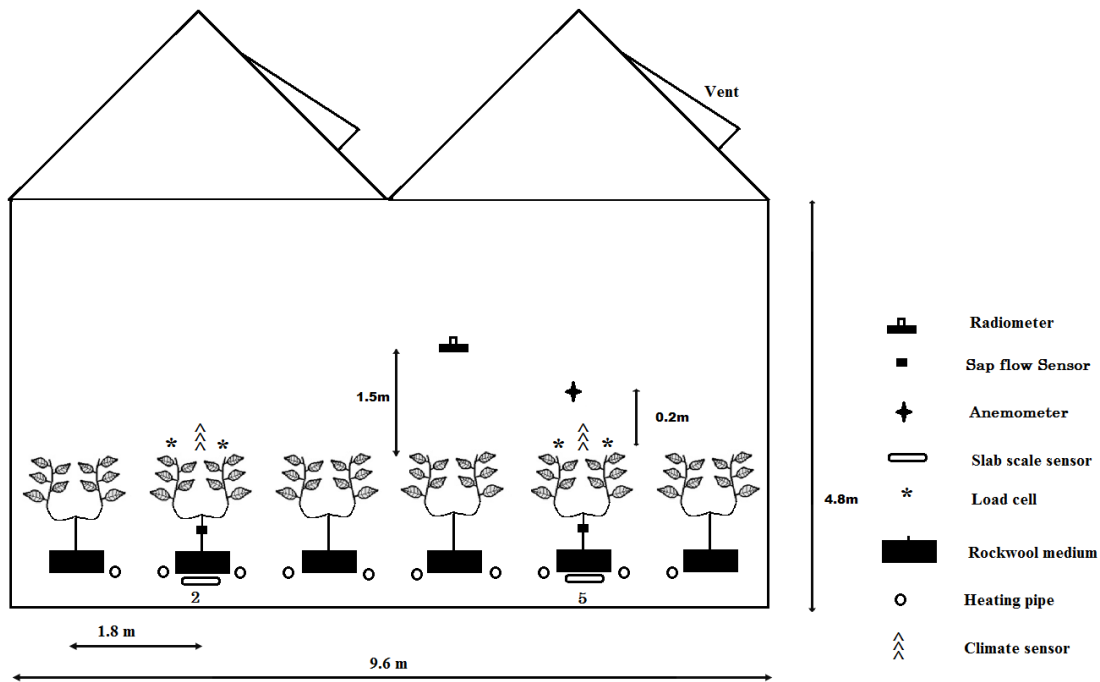


Figure 2, Overview of the greenhouse and the installed sensors, row 2 and 5 are indicated. The anemometer and radiometer are located 0.2m and 1.5m above the canopy respectively. The microclimate sensor is installed in between the top leaves of the crop.

3.3 Measuring Equipment Greenhouse Meteorological Data

To determine the effect of wind speed (u) on transpiration an ultrasonic anemometer is installed 0.2 m above the canopy. This allows monitoring of the air movement inside the greenhouse created by opening ventilation windows (Figure 2). The long- and short-wave radiation inside the greenhouse is measured with a radiometer 1.5 m above the canopy. The radiation sensor converts this measurement in a value for the net radiation (R_n). The leaf surface temperature (T_w) is measured using an optical temperature sensor connected to the microclimate sensor. Air temperature (T), and relative humidity (RH) are measured by two automatic microclimate sensors (Table 2).

Table 2, list of used measuring equipment

Sensor	Make & Model
3D sonic anemometer	Young Meteorological Instruments Model 81000 Sensitivity: 0.01 ms^{-1}
Load cell	Zemic Europe Type 1B-S Miniature Sensor
Slab scale	Wireless Value
Sap flow sensor	2grow
Microclimate sensor	30 Mhz
Leaf surface temperature	Optical temperature sensor 30Mhz
Irrigation sensor	Priva
Drain sensor	Priva level
Radiometer	Knipp & Zonen CNR4 Net radiometer Sensitivity: $5 \text{ to } 20 \mu\text{V W}^{-1} \text{ m}^{-2}$

3.4 Tomato Crop Transpiration Measurement

The measured transpiration is quantified for two different rows of plants, row 2 and row 5 (Figure 2). For the comparison with the transpiration models the mean value of these two rows is used, since the sensors used in the models are located in between row 2 and row 5. The measured transpiration is quantified in Python, version 3.8 with a water balance method (Equation 10).

$$\frac{dS}{dt} = Q_{in} - Q_{out} \quad (10)$$

With: S Water storage [L^3]
 Q Water flux [L^3h^{-1}]

The tomato crop is grown in rockwool slab covered with plastic, therefore there is no water exchange from the rootzone to the atmosphere, thus preventing evaporation. The water received by the plant is supplied directly to the rockwool medium via drip irrigation. Part of the irrigation water is drained, with the goal of flushing excess salts and nutrients from the rootzone. The irrigation flux ($Q_{Irrigation}$) therefore is a sum of the drain (Q_{drain}), water absorption by the plant (Q_{plant}), and water storage in the rockwool slab (S_{slab})(Equation 11).

$$Q_{Irrigation} = Q_{Drain} + Q_{Plant} + \frac{dS_{slab}}{dt} \quad (11)$$

With: S Water storage [L^3]
 Q Water flux [L^3h^{-1}]

The change in water storage ($\frac{dS_{slab}}{dt}$) in the rockwool slab is measured with slab scales. There is a slab scale both in row 2 and 5. Each scale measures the mass of two rockwool slabs, six pairs of roots, and the water present. The mass of the rockwool is constant over time. Since the plant is mature the change in mass of the organic material in the roots during the experiment is negligibly small.

The change in water storage in the plant is measured with load cells. These load cells measure the mass of the organic material and the water inside the plant. The weighted average water content between the fruits and plant material is measured at the end of the experiment and was found to be 93%. The density of water changes with temperature but this effect very small and thus neglected since the temperature changes between 15 and 35 °C. Therefore the change in mass is equal to the change in water storage.

The tomato crop takes up water and dissolved nutrients from the rockwool medium through their roots. The water is transported upward towards the leaves, where most of it leaves the plant as water vapour. Thus the change in water storage in the plant is the difference between the water absorption and the transpiration (Equation 12).

$$\frac{dS_{plant}}{dt} = Q_{Plant} - Q_{Transpiration} \quad (12)$$

With: S Water storage [L^3]
 Q Water flux [L^3h^{-1}]

Since the drain is only measured at the end of the day there is a need for higher resolution data. The water take up by the plant is simultaneously measured by 4 sap flow sensors. These provide high resolution data by measuring the temperature of the sap in a single plant stem, giving a heat impulse and measuring the temperature again a few centimetre further towards the leaves. The values measured by the sensor are an indication for the pattern of the water uptake by the plant, but do not have a unit. The relation between the sap flow and the water uptake is determined daily by comparing its daily total with the cumulative measurements from the slab scales. This relation is used to go from relative values to a unit of litre per hour per meter squared. Since the sap flow sensors measure the stem below the foliage, the water flow measured here is equal to the total water uptake by the plant.

3.5 Data Filtering

Data used in this study is collected from 2021-06-18 until 2021-09-14. During this time the sensors have sometimes not given a reading for an unknown reason. Therefore, the data contains missing and incorrect values that need to be filtered out. In the transpiration measurement missing values are very rare and filled in using linear interpolation.

The data for the transpiration models has several consecutive missing days. This data is left out, as daily values vary a lot based on the climate conditions and it is unknown what the correct values would be. The corrupt dates are 2021-07-17, the date range 2021-08-14 to 2021-08-18, and 2021-08-31.

For the comparison of transpiration models the use of an hourly timestep was chosen, as extremes and delays in the measurements are smoothed out. This is particularly relevant for the irrigation and drainage sensor, because there is uncertainty about the accuracy of these sensors. Analysing the data at a lower resolution makes the outcomes of the models less sensitive to extreme values.

3.6 Methods Used to Determine Model Accuracy

In this study four ways to compare the different models are presented. Firstly, the measured and modelled transpiration are compared by presenting the outcomes of the models compared to the measurement during two consecutive days in June (section 4.2.1). The second comparison uses linear regression and calculates the coefficient of determination (R^2) *for the hourly data of the entire experiment* (section 4.2.2). Thirdly, the cumulative transpiration over the total time of the experiment is calculated and compared (section 4.2.3). Fourthly, the absolute errors of the models *compared to the measurements* is plotted in a probability density function. Additionally the mean, standard deviations, skewness and kurtosis of this error are calculated for each model (section 4.2.4).

In this paper the absolute *error* is defined as the difference between the modelled and measured transpiration (Equation 13).

$$\varepsilon = E_{mod} - E_{mea} \quad (13)$$

A sensitivity analysis quantifies how a model (output) is affected by changes in the independent variables (input). The results of this analysis can be used to determine the required accuracy of the climate parameter measurements (Debnath, Adamala, & Raghuwanshi, 2015). In addition, it can be used to indicate which parameters are needed in the best performing models. The performed analysis evaluates the transpiration models response to changes in the climate parameters, net radiation (Rn), temperature (T), wind speed (u), and relative humidity (RH) (Table 4). The different input parameters each exert a different influence on transpiration.

The first method to calculate the sensitivity of the models, is by taking the mean values over time of the climate parameters and comparing this value to the solution found with a 10% increase or decrease in of one of the climate parameters. The second method is performed by increasing the climate parameters from the minimum to the maximum observed value while keeping other model input parameters constant. The constant values are chosen to be calculated by taking the mean value over the complete time series. The different scenarios are hypothetical, as the combination of climate parameters may have never been observed or taken place simultaneously.

4 Results

4.1 Evaluation of Aerodynamic and Internal Resistances

According to (Stanghellini, 1987), aerodynamic resistance inside a greenhouse is fairly constant because wind speed variations are small. Therefore different studies used a constant value for the aerodynamic resistance (Villarreal-Guerrero et al., 2012; (Morile et al., 2013; Gong et al., 2017). In an attempt to improve the transpiration models' accuracy, this study used the wind speed in Equation 5 and 7 to determine the aerodynamic resistances for the Penman-Monteith and Stanghellini models respectively. The results are presented in Figure 3 and Figure 4.

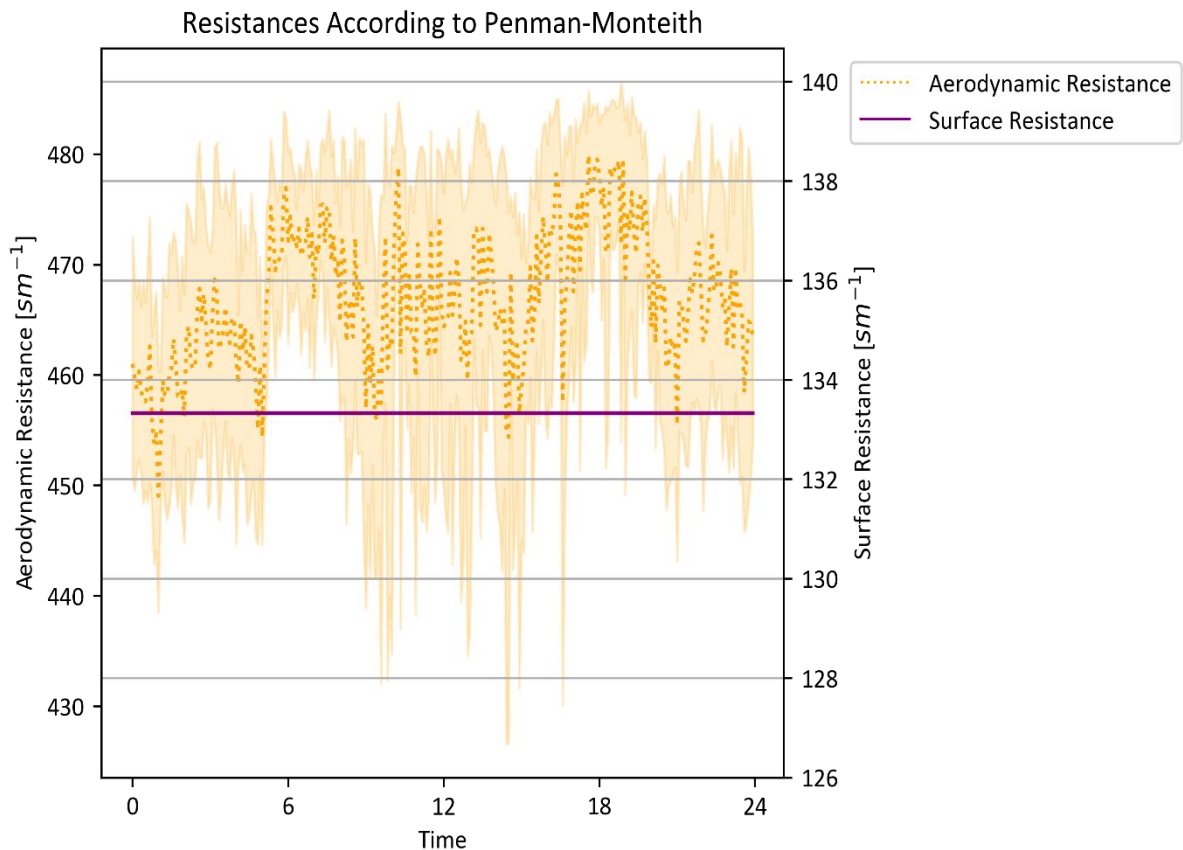


Figure 3, Hourly behaviour of the resistances in the Penman-Monteith model. Aerodynamic resistance is calculated using (Equation 5) and surface resistance is calculated using (Equation 6). The lines represent the mean values over the total time of the experiment for different times of the day. The 95% confidence interval is plotted in orange. The surface resistance is constant over time because of a simplification that uses a constant stomatal resistance found in literature (Equation 6). In reality this resistance is actively influenced by the plant and dependent on water availability and surface temperatures of the leaves.

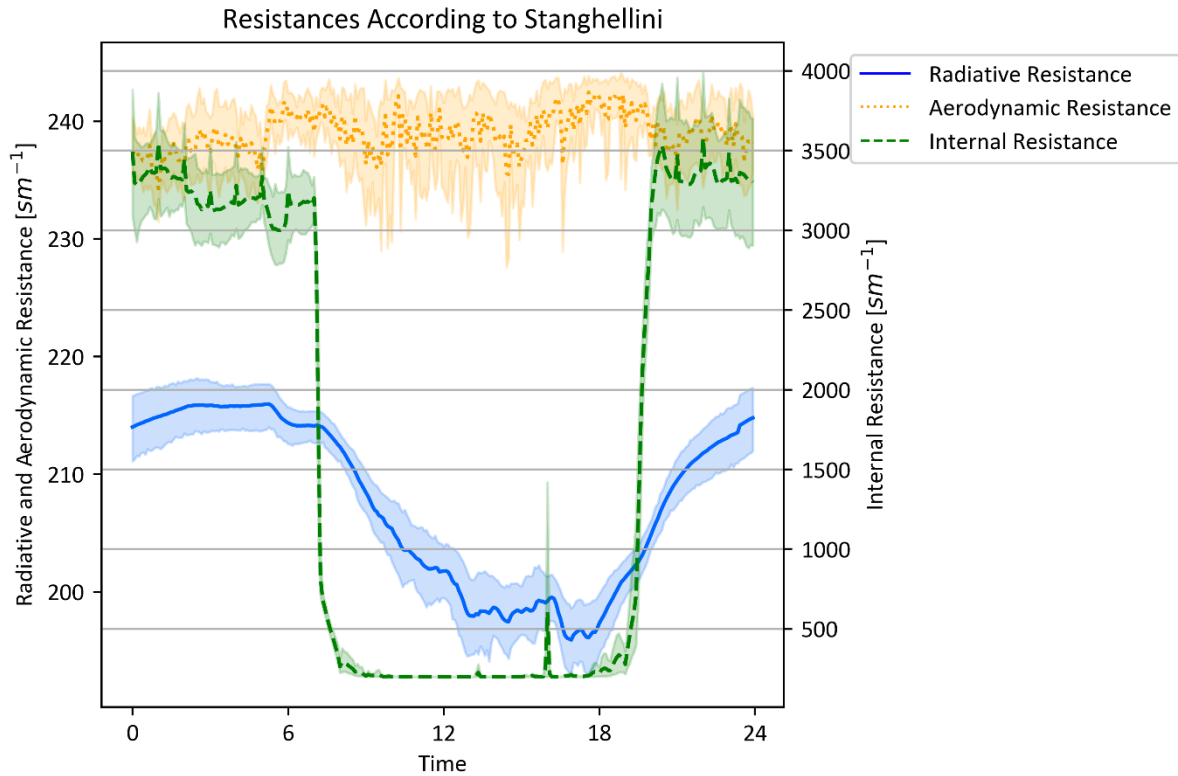


Figure 4, Hourly behaviour of the resistances in the Stanghellini model. Aerodynamic resistance is calculated using (Equation 7), internal resistance is calculated using (Equation 8), and radiative resistance is calculated using (Equation 9). The lines represent the mean values over the total time of the experiment for different times of the day. The 95% confidence interval is plotted in the same colour.

Results indicate that the average aerodynamic resistance for Penman-Monteith is $467 \text{ [sm}^{-1}\text{]}$, while the surface resistance is constant at $133 \text{ [sm}^{-1}\text{]}$ (Figure 3). Allen *et al.*, (1998) published a paper presenting the Penman-Monteith equation for estimating transpiration, recommending the use of standard values for a hypothetical grass reference surface having an assumed crop height of 0.12 [m] , a constant surface resistance of $70 \text{ [sm}^{-1}\text{]}$. The results indicate that the constant term used for stomatal resistance (r_i) of $200 \text{ [sm}^{-1}\text{]}$ in Equation 6 is too high for the climate conditions in this experiment and thus leading to the high value of $133 \text{ [sm}^{-1}\text{]}$ for the surface resistance.

The average aerodynamic resistance for the Stanghellini model is $239 \text{ [sm}^{-1}\text{]}$, with values varying between 199 and 245 (Figure 4). These values are slightly higher than the average values reported by (Stanghellini, 1987), (Villarreal-Guerrero, et al., 2012) and (Acquah, et al., 2018), who reported average values of 200, 185 and $145 \text{ [sm}^{-1}\text{]}$ respectively. Figure 4 shows that the internal and radiative resistances show strong diurnal behaviour, with average values of 1580 and $206 \text{ [sm}^{-1}\text{]}$ respectively. This is consistent with the values reported for tomato in (Stanghellini, 1987) and similar to the plant behaviour of cucumber as described in (Yan, et al., 2020). Note that the internal resistance is consistently higher than the aerodynamic resistance which is in agreement with findings from (Acquah, et al., 2018) for tomatoes in a greenhouse with natural ventilation.

4.2 Accuracy of the Transpiration Modelling

4.2.1 Time Series

The first comparison between the different models and the transpiration measurement is made with a time series over two consecutive days in June. The days are randomly chosen and represent typical behaviour of the models. Figure 5 shows the measured radiation during these days, where June 21st is a day with cloud cover, and June 22nd a day with alternately sunshine and clouds.

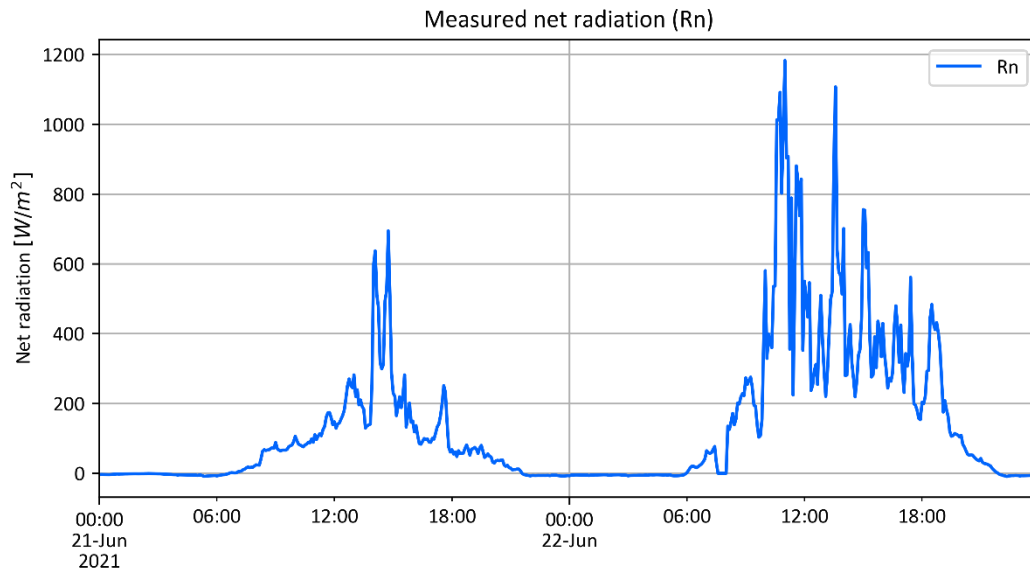


Figure 5, Diurnal variations in net radiation measurements on the 21st and 22nd of June. The resolution of the data is 5 minutes.

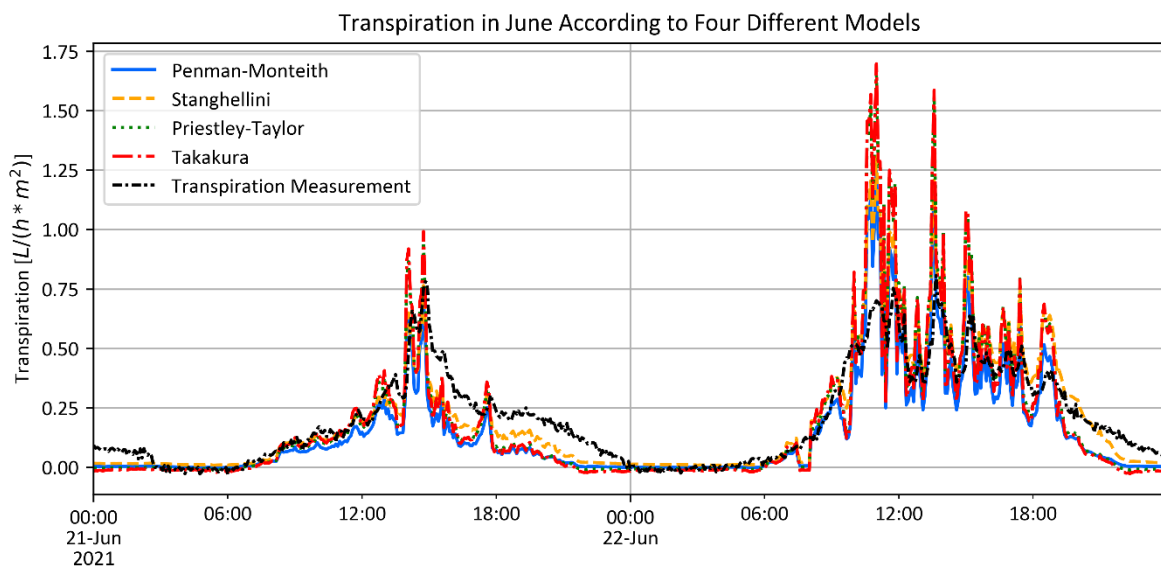


Figure 6, Diurnal variations in transpiration of four different models and the transpiration measurement on the 21st and 22nd of June. The resolution of the data is 5 minutes.

Figure 6 shows the variations in transpiration during the day, where it is apparent that all models overestimate the transpiration during the day when the radiation is large. In order to investigate this behaviour and make sure this isn't a unique event the mean transpiration of the four models compared to the transpiration measurement is presented in (Figure 7-10).

When comparing transpiration measurements to modelled values it is found that the transpiration in the greenhouse continues several hours after the sun has set (Figure 7-10). The models are not able to accurately calculate the transpiration when the net radiation is declining. This behaviour and possible explanations is described in the discussion (Section 5).

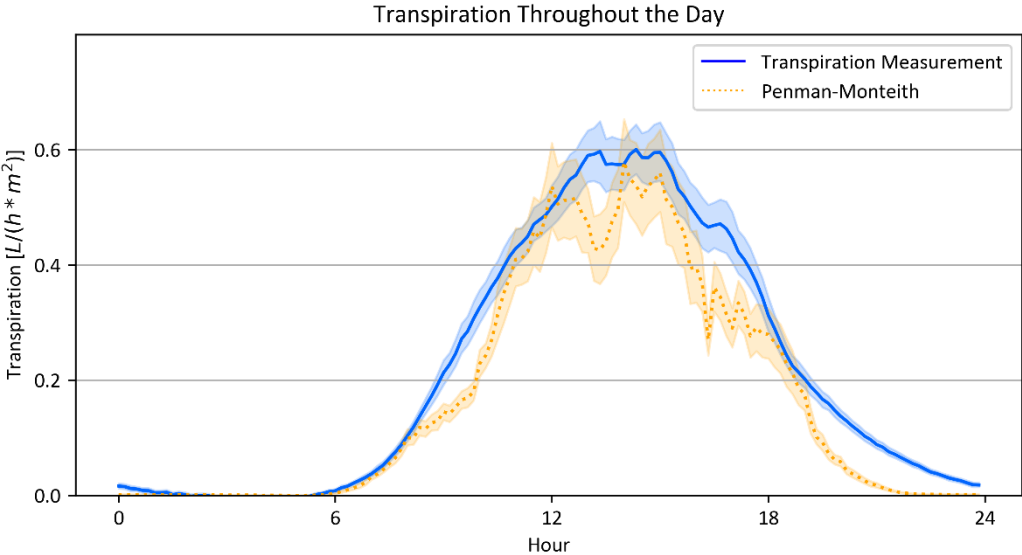


Figure 7, Comparison between mean values of transpiration measurements vs Penman-Monteith model. The lines represent the mean values over the total time of the experiment for different times of the day. The 95% confidence interval is plotted in the same colour. The resolution of the data is 5 minutes.

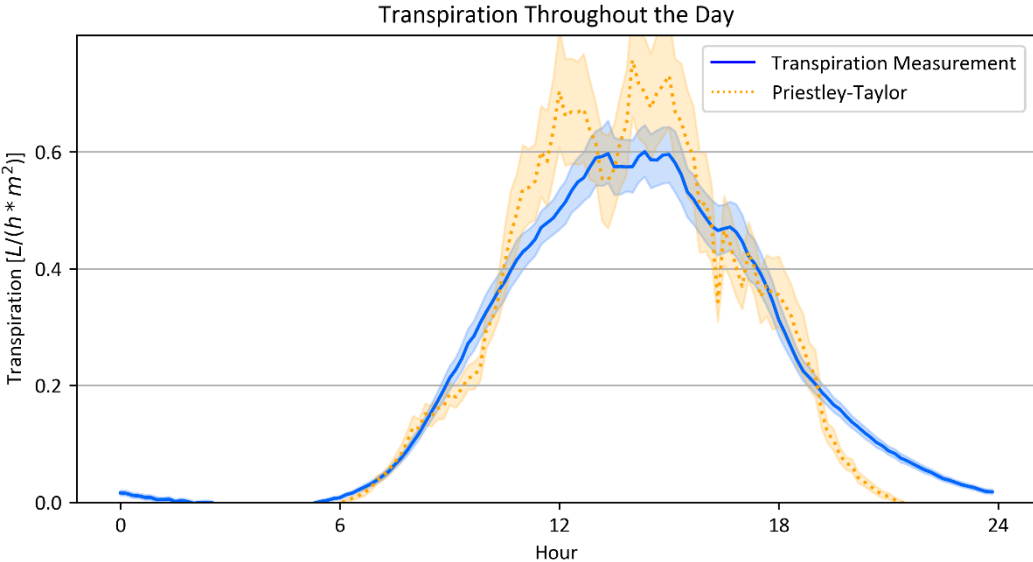


Figure 8, Comparison between mean values of transpiration measurements vs Priestley-Taylor model. The lines represent the mean values over the total time of the experiment for different times of the day. The 95% confidence interval is plotted in the same colour. The resolution of the data is 5 minutes.

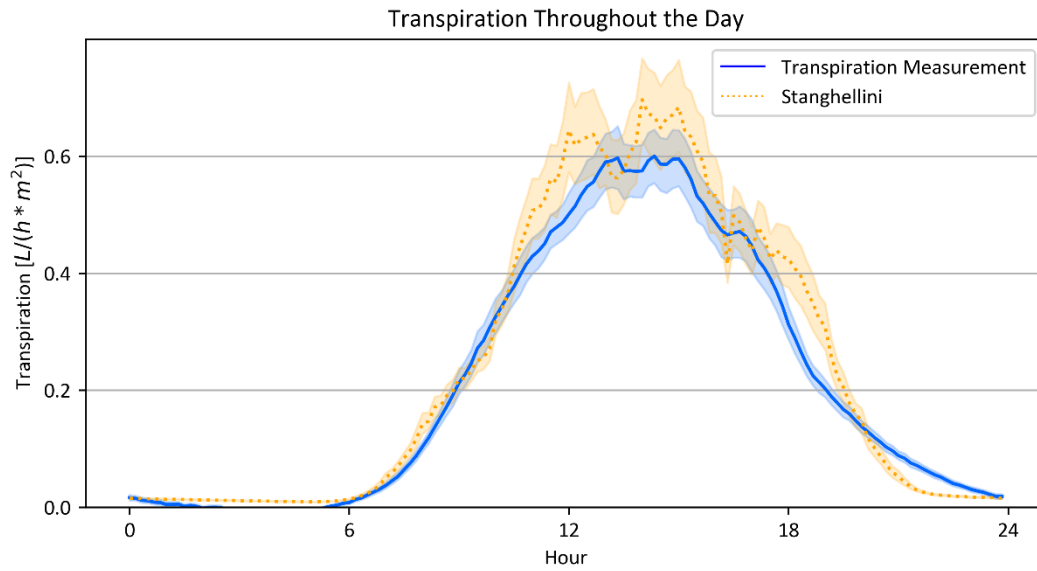


Figure 9, Comparison between mean values of transpiration measurements vs Stanghellini model. The lines represent the mean values over the total time of the experiment for different times of the day. The 95% confidence interval is plotted in the same colour. The resolution of the data is 5 minutes.

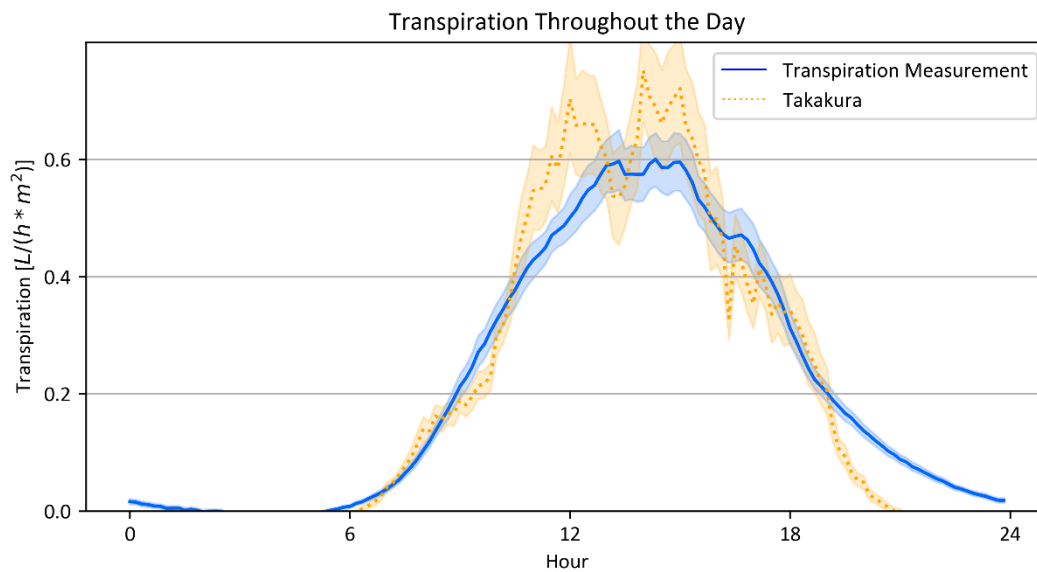


Figure 10, Comparison between mean values of transpiration measurements vs Takakura model. The lines represent the mean values over the total time of the experiment for different times of the day. The 95% confidence interval is plotted in the same colour. The resolution of the data is 5 minutes.

4.2.2 Scatterplot Modelled vs Measured

The second method to analyse the accuracy of the transpiration modelling is plotting the modelled against the measured transpiration. A hypothetical perfect model would result in a linear regression ($x = y$), where the values for modelled and measured transpiration are equal.

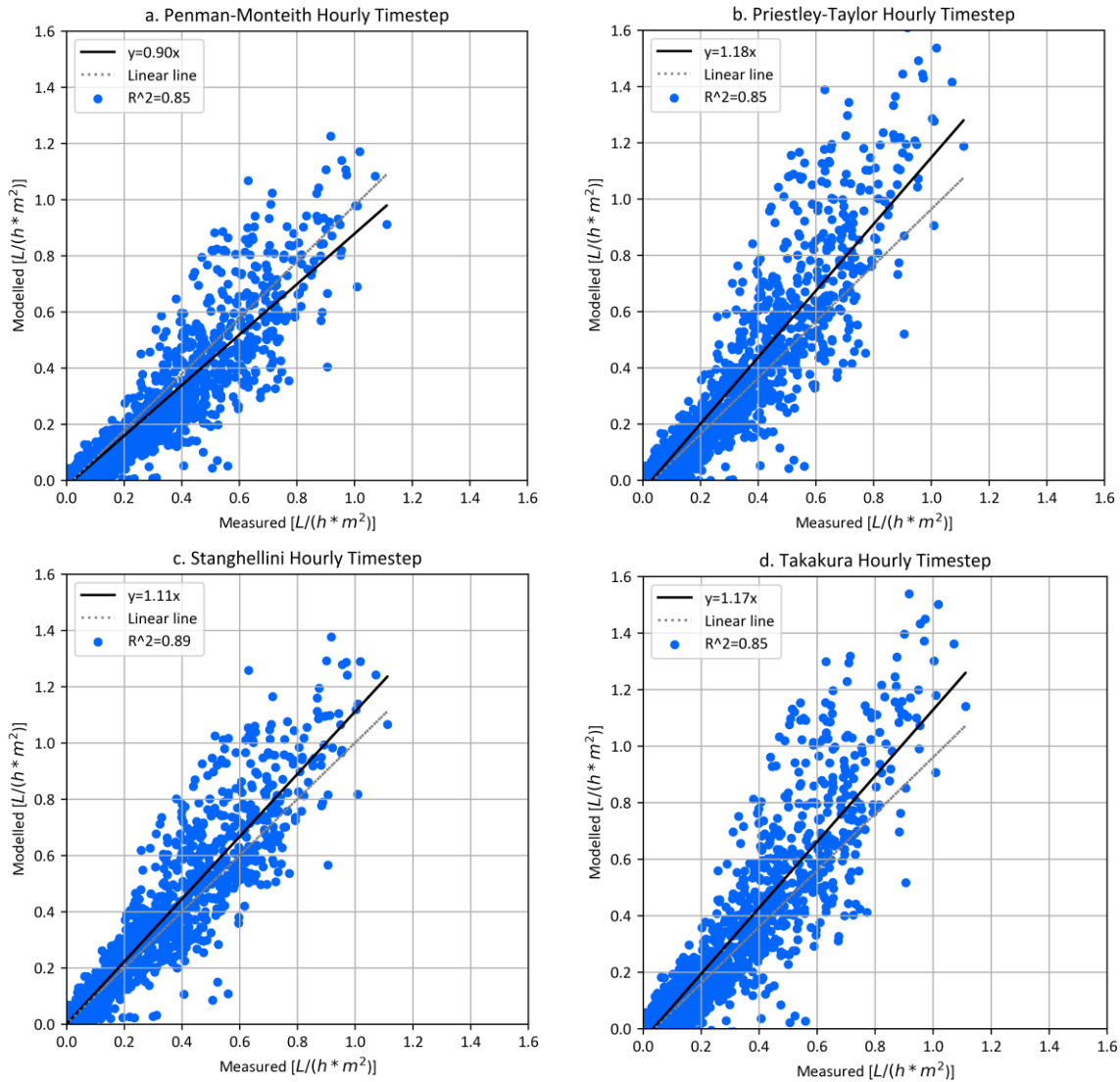


Figure 11, Comparison between the measured hourly transpiration and modelled transpiration according to four different transpiration models: a) Penman-Monteith, b) Priestley-Taylor, c) Stanghellini, d) Takakura. The data of the entire experiment is used.

Figure 11a shows the comparison between measured and calculated transpiration for the Penman-Monteith model. The regression line is close to 1:1, which indicates a high correlation between measured and calculated transpiration. The coefficient of determination (R^2) is 0.85. Note that the slope of the regression line is 10% lower than 1, indicating that the model will generally underestimate the transpiration. While the Penman-Monteith model is recommended by the US Food and Agriculture Organization, (Widmoser, 2009) found that errors compared to measurements can range from -9% to 40%.

Figure 11b, shows that Priestley-Taylor has a coefficient of determination ($R^2=0.85$). Figure 11c, shows the comparison between measured and calculated transpiration for the Stanghellini model. With 0.89 the coefficient of determination (R^2) is the highest between the four models. This is in accordance with the findings of (Pamungkas et al., 2014), who reported that for the calculation of tomato transpiration in soilless greenhouse the Stanghellini model is most suitable. The slope of the regression line is 11% higher than 1. Figure 11d, shows that Takakura has a coefficient of determination ($R^2=0.85$).

In all four models there is a tendency to have more extremes towards higher transpiration values. At these high levels of transpiration, the transpiration values in the models are more likely to be higher than the measurements, indicated by the fact that there are more points above the regression line. At lower transpiration values the modelled values generally are lower than the measurements.

4.2.3 Error Density Distribution

Figure 12 shows the probability density function of the error. The higher the graph, the more frequent the occurrence. Probability density distributions only apply to continuous variables and the probability for any single error is defined as zero (Kim et al., 2019). The surface area under the graphs is equal to 1, as this represents all different datapoints.

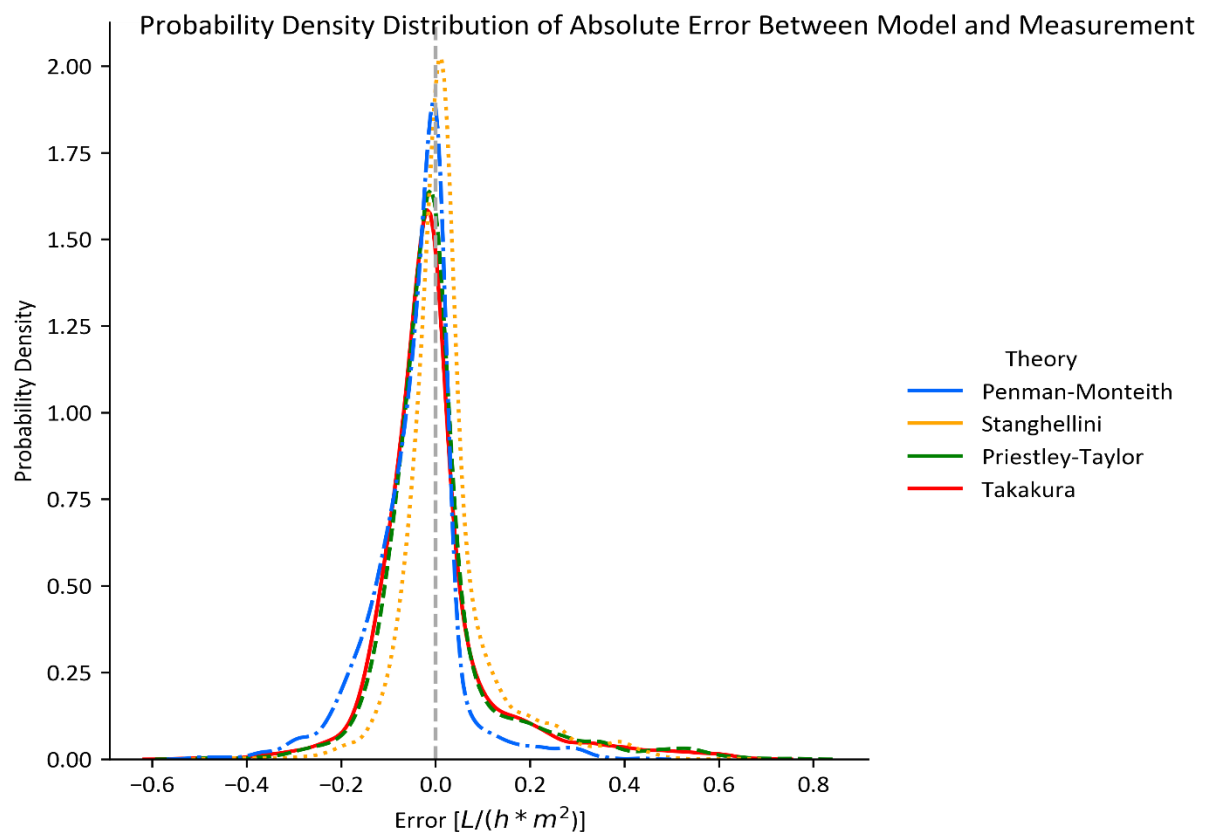


Figure 12, Probability density distribution of the absolute error between the modelled and measured transpiration in hourly resolution. A value lower than 0 indicates an underestimation, while a value higher than 0 indicates an overestimation.

The results indicate that 95% of the time the absolute error of the Penman-Monteith model is in the range of -0.25 to 0.16 [$L / (h * m^2)$]. The 95% confidence interval for the Stanghellini model is -0.13 to 0.31 [$L / (h * m^2)$]. The 95% confidence interval for the Priestley-Taylor model is -0.18 to 0.38 [$L / (h * m^2)$]. The 95% confidence interval for the Takakura model is -0.19 to 0.38 [$L / (h * m^2)$]. When compared to the average hourly transpiration of 0.21 [$L / (h * m^2)$] this error can be considered large.

Table 3, Mean error [L / (h * m²)], Standard deviation [L / (h * m²)], Skewness, and Kurtosis of the error probability density distribution referring to (Figure 12).

Model:	Mean Error [L / (h * m²)]	Standard Deviation [L / (h * m²)]	Skewness [-]	Kurtosis [-]
Penman-Monteith	-0.034	0.094	0.220	4.626
Priestley-Taylor	0.004	0.127	1.899	6.660
Stanghellini	0.025	0.099	1.422	5.297
Takakura	-0.003	0.126	1.698	6.163

Mean is the average value of the distribution. When this value differs from zero this indicates a bias, or systematic error in the model. Table 3 presents that the Penman-Monteith model has a negative bias (0.034 [L / (h * m²)]) indicating that the model underestimates transpiration, whereas the Stanghellini model has a positive bias (0.025 [L / (h * m²)]) indicating that the model generally overestimates transpiration. For the Priestley-Taylor and Takakura models the bias is very small.

Standard deviation is a measure of the amount of variation in a set of values. Table 3 presents that the Priestley-Taylor and Takakura models have a larger standard deviation compared to Stanghellini and Penman-Monteith. Indicating that the errors in these models are larger.

Skewness is a measure of the probability distributions symmetry. The skewness for all models can best be described as slightly positively skewed, represented by a distribution with a larger tail in the positive direction. This is in accordance with the findings in section 4.2.2 and means that extremes that overestimate the transpiration are more likely. Note that since the error distribution is somewhat symmetrical around zero, the modelled transpiration can either be higher or lower than the measured value.

Kurtosis is a measure of the 'tailedness' relative to a normal distribution. This study uses Fisher's definition of kurtosis, giving the normal distribution a kurtosis of 0. A kurtosis value larger than zero indicates a leptokurtic distribution with fewer extreme values than a normal distribution. All models have a large positive kurtosis, corresponding with distributions with values either near the mean or at rare extremes (Table 3). It was found that all models have a strong peak in the probability density distribution, meaning that errors close to zero are most common.

4.2.4 Cumulative Transpiration

The fourth method to analyse the accuracy of the transpiration modelling is calculating the cumulative transpiration for the different models (Figure 13). Days with measurement errors are left out, thus the actual cumulative transpiration at the end of the experiment on September 15th was higher. This also means that any differences between the models and measurements at the end of the time series are underestimated.

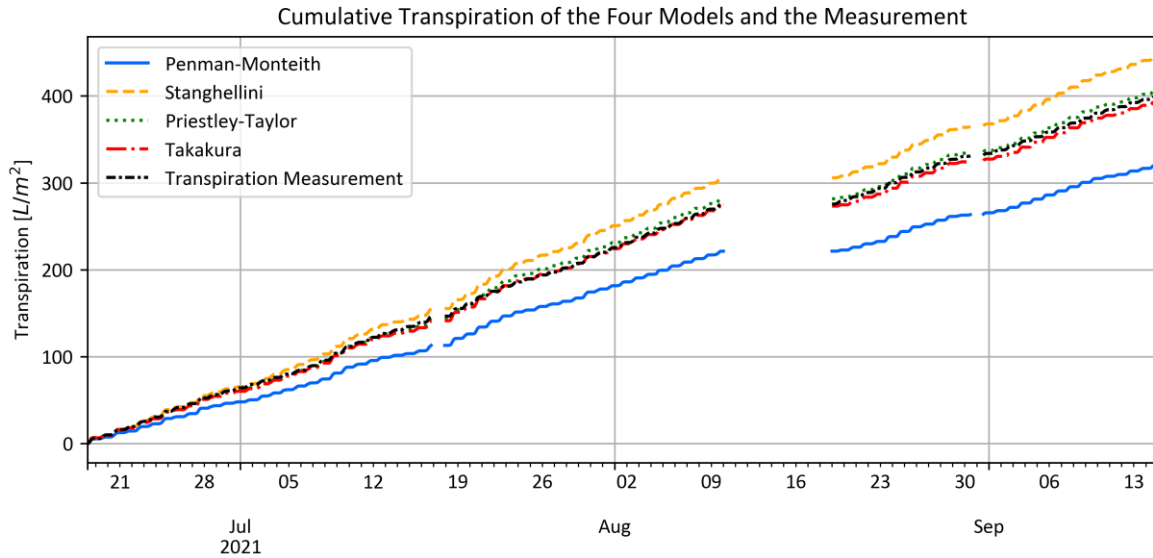


Figure 13, Cumulative transpiration of the modelled and measured transpiration in hourly time step.

Figure 13 shows that all four models follow the same trend as the measured transpiration, where days with lower transpiration result in a decrease in the slope of the curves and days with high transpiration result in an increase in the slope. Over the experiment from June to September there is no indication of seasonality as the slopes in the different months are similar.

At the end of the experiment the measured cumulative transpiration is 400 [L/m²]. Figure 13 shows that using the Penman-Monteith model, with a maximum value of 336 [L/m²], results in an underestimation of the transpiration. While the Stanghellini model, with a maximum value of 445 [L/m²], results in an overestimation. The Priestley-Taylor and Takakura models perform the best in this test, with slightly higher (406 L/m²) and lower (394 L/m²) values respectively.

4.3 Individual Parameter Sensitivity of the Transpiration Models

Higher parameter sensitivity of a model suggest that a small change in the climate parameter results in a larger change in the transpiration calculation. In other words an error in the more sensitive measured input parameters results in a larger error in the transpiration calculation. Thus it is most important to measure the sensitive climate parameters correctly.

Section 4.3.1 presents the effects of a percentual change in climate parameters, while section 4.3.2 presents a scenario distribution where the sensitivity of the climate parameters is evaluated over the range of observed values.

4.3.1 10% Change Table

Table 4, illustrates the first sensitivity test for modelled transpiration, calculated by taking the mean values over time of the climate parameters and comparing this value to the solution found with a 10% increase or decrease in of one of the climate parameters.

Table 4, Sensitivity of the different parameters. The table presents what happens with the transpiration when an input parameter is increased or decreased with 10% from its mean value. The mean value of net radiation (Rn) is 160 [W/m²]. The mean value of temperature (T) is 22.4 [°C]. The mean value of wind speed (u) is 0.05 [m/s]. The mean value of relative humidity (RH) is 76.6 [%]. Some cells are left empty because these climate parameters are not included in these models.

model	Modelled Transpiration [W/m ²]	Change Rn -10%	Change Rn +10%	Change T -10%	Change T +10%	Change u -10%	Change u +10%	Change RH -10%	Change RH +10%
Penman-Monteith	125.2	-9.4 %	9.4 %	-3.4 %	3.1 %	0.0 %	-0.0 %	1.7 %	-1.7 %
Priestley-Taylor	151.8	-10.0 %	10.0 %	-3.5 %	3.2 %				
Stanghellini	164.8	-6.3 %	6.2 %	-1.1 %	0.9 %	0.0 %	-0.0 %	9.8 %	-9.8 %
Takakura	142.9	-11.2 %	11.2 %	10.7 %	-10.7 %				

Across the four models the transpiration in the greenhouse is primarily affected by an increase in net radiation (Table 4). A 10% change in net radiation leads to a 9.4% change in the outcome of the Penman-Monteith model, a 10% change for Priestley-Taylor, a 6.3% change for Stanghellini, and a 11.2% change for Takakura. Radiation is the largest energy source in the greenhouse and can change large quantities of liquid water inside the leaves into water vapour. An increase in net radiation by more sunshine or artificial light use in the greenhouse will increase transpiration and vice versa.

The transpiration is affected by the ambient air temperature since a temperature increase leads to a higher capacity of the air to hold water vapor. The Takakura model is very sensitive to temperature changes compared to the other models. This can be explained by the form of the equation where the transpiration is equal to the net radiation minus temperature variations (Equation 4). It must be noted that this value is strongly exaggerated because the leaf surface temperature is not changed while the air temperature is, something that is not realistic in a greenhouse.

Interesting to note is that the Stanghellini model is very sensitive to relative humidity. This is explained by the fact that in the model the vapour pressure deficit is multiplied by the LAI, thus amplifying its effect on the outcome (Equation 2).

The wind speed inside the greenhouse has the lowest effect on the transpiration, with an effect smaller than 0.0% for a 10% change. This is in agreement with the findings from (Tabari & Talaee, 2014) who found that the sensitivity of wind speed and temperature was lower in more humid climate conditions. The wind replaces the saturated air around the leaves and removes heat, when the relative humidity in the greenhouse is higher this process is less effective, and thus the effect on transpiration is smaller.

According to Debnath *et al.* (2015) different sites and climates have significant variations in the sensitivity of transpiration. The researchers found considerable fluctuations over the season and the amplitude of the same climate parameters showed variations among different sites. Therefore the findings in sensitivity for this greenhouse cannot directly be extrapolated to other locations.

4.3.2 Scenario Distribution

The second sensitivity test for modelled transpiration is presented in (Figures 14-17). When investigating the parameter under review all other input parameters are set to a constant default value. These constant values are chosen to be calculated by taking the mean value over the complete time series.

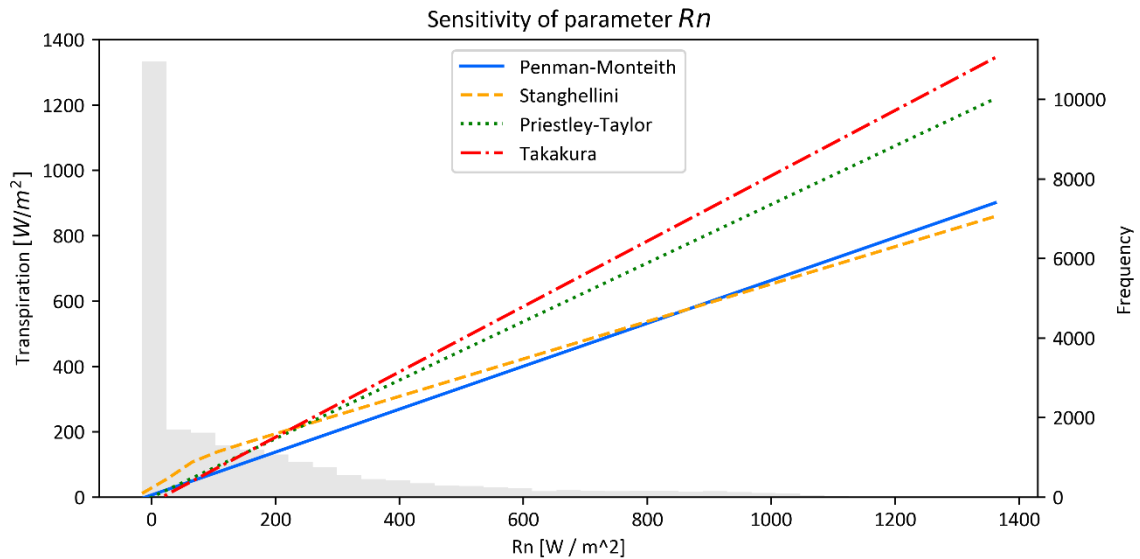


Figure 14, Sensitivity of the net radiation. The net radiation is measured 1m above the canopy with a frequency of 5 minutes. The frequency of different radiation values is presented in a histogram in the background, the mean is 160 [W/m²].

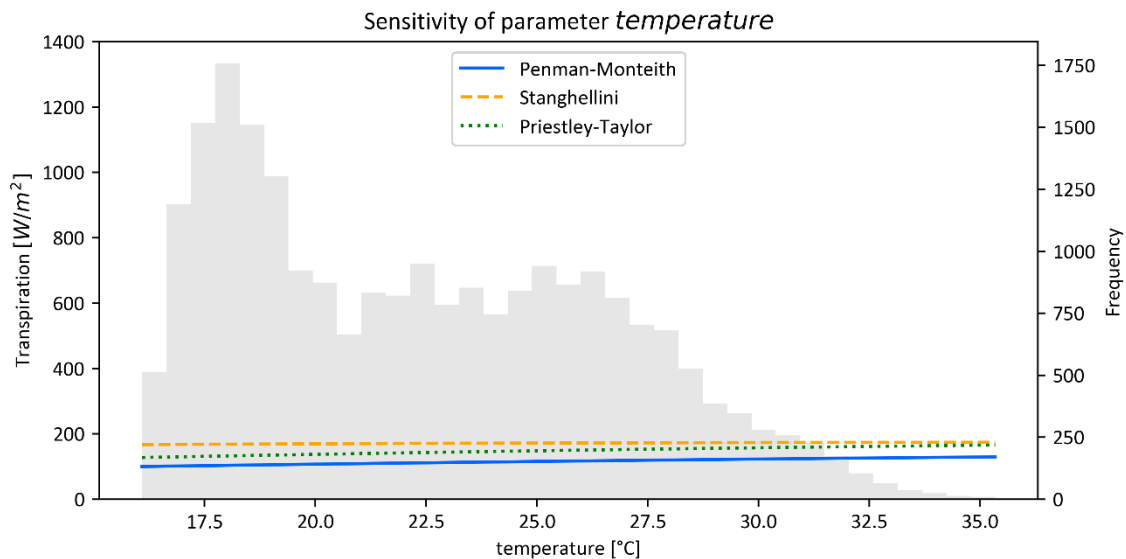


Figure 15, Sensitivity of the air temperature. The temperature is measured in the top of the canopy with a frequency of 5 minutes. The frequency of different temperature values is presented in a histogram in the background, the mean is 22.4 [°C]. Takakura is excluded because this model is sensitive to both air temperature and surface temperature, thus analysing the sensitivity to just air temperature is incorrect.

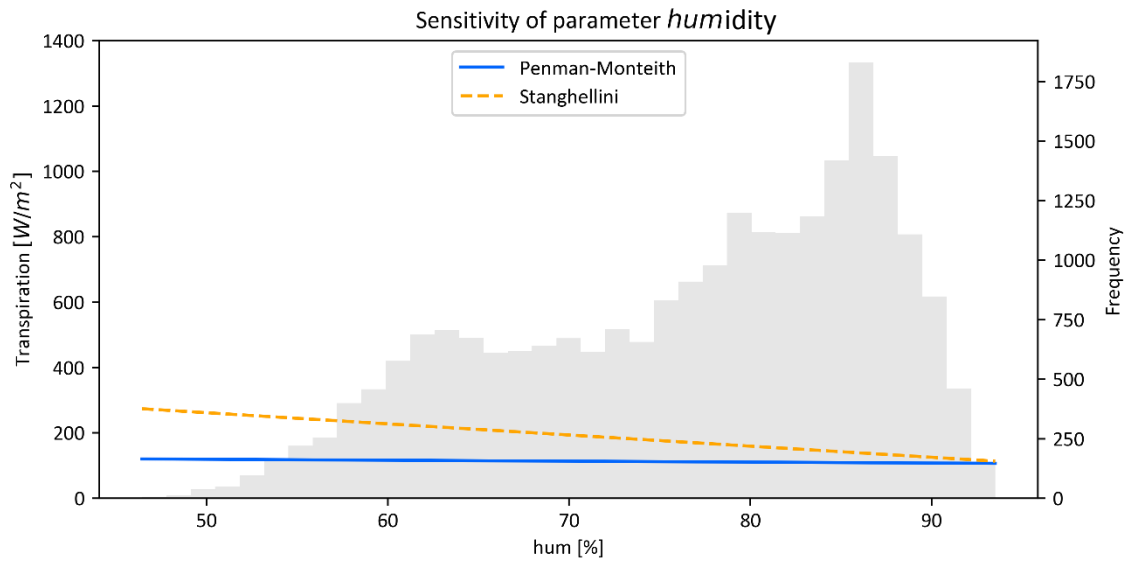


Figure 16, Sensitivity of the parameter relative air humidity. The humidity is measured in the top of the canopy with a frequency of 5 minutes. The frequency of different humidity values is presented in a histogram in the background, the mean is 76.6 [%]. The Priestley-Taylor and Takakura models are excluded as these do not include relative humidity.

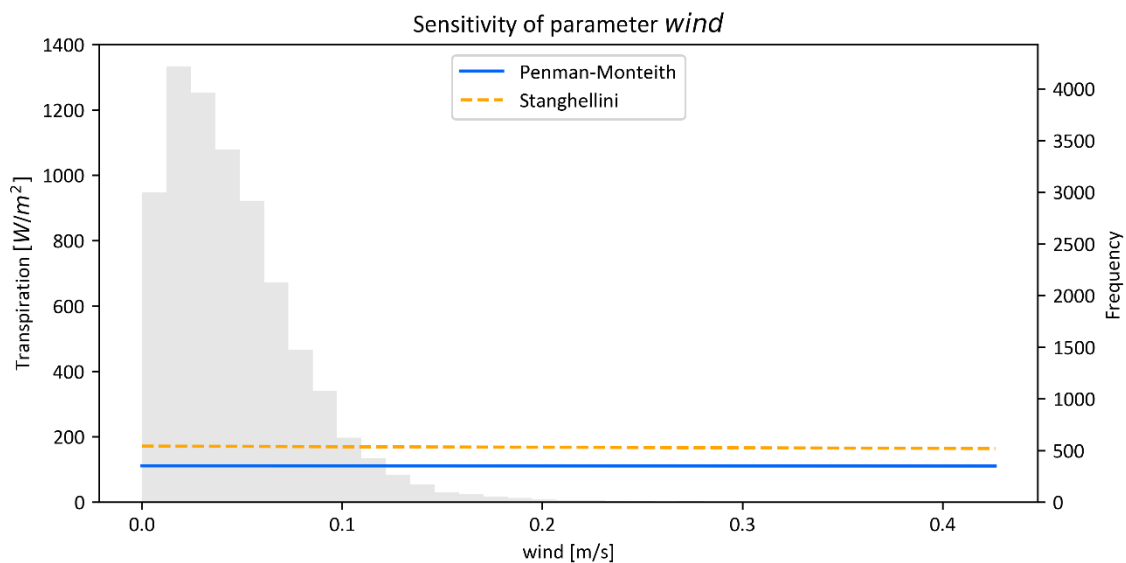


Figure 17, Sensitivity of the parameter wind speed. The wind speed is measured 0.2m above the canopy with a frequency of 5 minutes. The frequency of different wind speed values is presented in a histogram in the background, the mean is 0.05 m/s. The Priestley-Taylor and Takakura models are excluded as these do not include wind speed.

A positive slope indicates an increase in transpiration values with an increase in the climate parameter under review. The sensitivity is displayed on the vertical-axis thus a larger spread between these values indicates a larger sensitivity. Thus it can be deduced that across the four models transpiration is most sensitive to the climate parameter net radiation, followed by temperature, relative humidity, and lastly wind speed.

When comparing the sensitivity of the transpiration models for the parameter net radiation, the highest sensitivity was found for Takakura, followed by Priestley-Taylor, Penman-Monteith, and Stanghellini (Figure 14). Interesting to note is that the Stanghellini model has a nonlinear relationship explained by the effect of radiation on internal resistance values. This results in a strong sensitivity for low values of net radiation, while the sensitivity reduces when moving to the maximum values.

When comparing the sensitivity of the transpiration models for the parameter relative humidity, it is found that the Stanghellini model is very sensitive to changes in relative air humidity compared to Penman-Monteith (Figure 16). This is explained by the fact that in the equation the vapour pressure deficit is multiplied by the LAI. Since the LAI is always positive and equal to 3, this amplifies the effect of relative humidity on the outcome of transpiration.

When comparing the sensitivity of the transpiration models for the parameter wind speed, it is found that a variation in wind speed in both the Stanghellini and Penman-Monteith model does not change the transpiration (Figure 17). Therefore we can conclude that the aerodynamic resistance inside the greenhouse is fairly constant, which is in accordance with the findings of (Acquah et al., 2018).

It must be noted that this result is calculated with a constant radiation and temperature. Therefore the radiative resistance that is dependent on radiation, and thus changes strongly during night and day, is reduced to an average mean value in this analysis. The same is true for the internal resistance that is dependent on temperature. A plot of the variations in internal resistance over the day is presented in (Figure 4).

5 Discussion

When comparing the behaviour of the mean transpiration calculated by the models to the mean measured transpiration, a striking difference between the morning and evening hours is found (Figure 7-10). Transpiration modelled per five minutes did not show a strong correlation with the transpiration measurements. The models show strong overshooting during the time of day when the net radiation is highest. This effect corresponds to the findings in literature, explaining that transpiration rates decline sharply when air temperatures and incoming radiation exceed a certain value (Stanghellini, 1987). The transpiration measurement during the second half of the day tends to be higher than the calculations by the different models, while the transpiration measurement tends to be lower in the middle of the day. The most likely explanation for this behaviour is that the modelled transpiration is first overestimated because incoming radiation is used for heating of the plants and greenhouse structure, and then underestimated due to extra release of energy during the evening hours.

A second explanation for this behaviour could be the simplification made in the models by assuming that the heat flux transmitted into the soil is zero. Estimations on how much energy is absorbed by the canopy depend strongly on greenhouse characteristics, and on the presence of climate control equipment (Katsoulas & Stanghellini, 2019). The energy available for the tomato canopy is the difference between the net radiation measured above the plants and the heat flux transmitted into the soil. The heat flux was assumed zero because the plants grow in slabs covered in white plastic, with a small surface area relative to the canopy. White has a high albedo making the heat storage low from incoming radiation low. However, the models do not take into account that the greenhouse has a heating system with iron heating pipes, radiating heat into both the growing slabs and the plants. Over a 24 hour period the effect on cumulative transpiration might be small, since the energy used to heat the surfaces is released as radiation on a later moment. However, for the hourly data used in this study this effect causes significant distortions.

Ignoring transpiration calculations during night-time is discouraged as this can be as much as 15% of the daily sum in arid and semiarid climates (Pereira et al., 2015).

Since it seems that the tomato crop cannot convert peak radiation into transpiration and instead this energy is used to heat the plant and greenhouse, it is interesting to know the stomatal behaviour during hours with peak radiation. Stomatal resistance during different times of day, can be estimated from diffusion porometer measurements (Gong et al., 2017; Villarreal-Guerrero et al., 2012). Different exponential relationships between leaf stomatal resistance and solar radiation are reported in the scientific literature (Bakker, 1991; Gong et al., 2017; Stanghellini, 1987). However, these relations are specific for the climate, greenhouse, and crop type, making them unsuitable for direct use in transpiration models.

This study used a constant stomatal resistance of 200 [sm^{-1}], and found this to be too high for the climate conditions during the experiment. Villarreal-Guerrero *et al.* (2012) reported difficulties obtaining reliable stomatal resistance readings from a diffusion porometer, and proposed calibrating the internal resistance to transpiration measurements before its use in the models of Penman-Monteith and Stanghellini. A study on tomato transpiration fluid dynamics inside a Venlo-type greenhouse in France proposed the use of a minimum stomatal resistance of 120 [sm^{-1}] that is adjusted based on the leaf surface temperature (Boulard et al., 2017). In further studies it is recommended to analyse the performance of the models when using a calibrated or measured stomatal resistance.

Specifically for the Stanghellini model the LAI was assumed to be constant over the experiment since the tomato crop was in a mature state. For this value 3 [$\text{m}^2 \text{m}^{-2}$] was used, as this was found in literature (Acquah et al., 2018; Stanghellini et al., 2019). Since this study found that the Stanghellini model is sensitive to changes in relative humidity and this climate parameter is multiplied by LAI, an accurate LAI value is important for transpiration calculations. Therefore in future studies, it is recommended to measure LAI with several non-destructive measurements of leaf dimensions during the experiment.

When comparing the coefficient of determination (R^2) of the four different models, it is found that the models perform with similar accuracy. This is in accordance with the findings of Villarreal-Guerrero *et al.* (2012), who found highest accuracy for the Stanghellini model but no significant difference between Penman-Monteith, Stanghellini, and Takakura. Since the Takakura model is much simpler to implement these researchers recommend this as the most practical for the use in cultivation.

In this study the microclimate is measured in between the top leaves of the crop (Figure 2), because it was reasoned that this is the part of the plant that the radiometer monitors. Other research compared the performance of the Stanghellini model at three different heights in cucumber crops (Yan et al., 2020). The highest accuracy in the Stanghellini model was found with microclimate data measured the lowest in the crop at 0.5m. The study used cucumbers, but these resemble tomatoes in cultivation. Therefore, it is suggested to repeat this study using microclimate sensors lower in the canopy in order to investigate if model accuracy can be improved.

6 Conclusions

This study set out to analyse the accuracy of four different models to estimate the transpiration of tomato plants inside a high-tech soilless greenhouse. During the summer a three month experiment was conducted in a Venlo-type greenhouse in The Netherlands. The tomato transpiration was measured using sap flow sensors and lysimeters. Hourly transpiration data was compared to Penman-Monteith, Stanghellini, Priestley-Taylor and Takakura models. The results show that the transpiration can be modelled by different transpiration models, however the errors are too large to make the outcomes useful for irrigation scheduling. Linear regression indicates that the most accurate model is Stanghellini with a coefficient of determination ($R^2=0.89$). Penman-Monteith ($R^2=0.85$), Priestley-Taylor ($R^2=0.85$), and Takakura ($R^2=0.85$) followed closely. The Penman-Monteith and Priestley-Taylor models, intended for outdoor use, have a similar accuracy as the Stanghellini and Takakura models that are developed for Venlo-type soilless greenhouse.

The Priestley-Taylor and Takakura models perform best in calculating the cumulative hourly transpiration over the three month period with an error of 6 [Lm^{-2}] out of a total 400 [Lm^{-2}]. The Stanghellini model overestimated the transpiration by 45 [Lm^{-2}] while Penman-Monteith underestimated the transpiration by 67 [Lm^{-2}]. An error density distribution shows that the Penman-Monteith model generally underestimates transpiration by 0.034 [$\text{Lm}^{-2}\text{h}^{-1}$], whereas the Stanghellini generally overestimates transpiration by 0.025 [$\text{Lm}^{-2}\text{h}^{-1}$]. For the Priestley-Taylor and Takakura models the bias is negligibly small. The range of the errors indicate that the most accurate model is Penman-Monteith with a 95% confidence interval between -0.25 and 0.16 [$\text{Lm}^{-2}\text{h}^{-1}$], closely followed by Stanghellini with -0.13 and 0.31 [$\text{Lm}^{-2}\text{h}^{-1}$]. The Priestley-Taylor and Takakura models perform worse with an error in the range of -0.18 to 0.38, and -0.19 to 0.38 [$\text{Lm}^{-2}\text{h}^{-1}$] 95% of the time. When compared to the average hourly transpiration of 0.21 [$\text{Lm}^{-2}\text{h}^{-1}$] this shows that the models are not accurate enough for irrigation scheduling. These results show that the Penman-Monteith and Stanghellini models that include two more observed climate variables compared to Priestley-Taylor and Takakura have a smaller error.

Most greenhouse climate and irrigation control computers available today are based on the measured outside solar radiation. Although the sensitivity analysis showed that net radiation is the climate parameter that influences transpiration the most, air temperature and relative humidity have significant influence on the outcome of transpiration models as well. Firstly, a 10% change in net radiation leads to a 9.4% change in transpiration calculated by the Penman-Monteith model, a 10% change for Priestley-Taylor, a 6.3% change for Stanghellini, and a 11.2% change for Takakura. Secondly, a 10% change in temperature leads to a 3.4% change in transpiration calculated by the Penman-Monteith model, a 1.1% change for Priestley-Taylor, a 3.5% change for Stanghellini, and a 10.7% change for Takakura. Thirdly, a 10% change in relative humidity leads to a 1.7% change in transpiration calculated by the Penman-Monteith model, and a 9.8% change for Stanghellini. Therefore, it is recommended to include air temperature and relative humidity in models used to estimate transpiration inside a greenhouse. It is found that variations in the wind speed inside a greenhouse do not result in significant changes in modelled transpiration. Increasing the wind speed by 10% results in 0.0% change in the transpiration.

The biggest challenge with the application of the resistance based Penman-Monteith and Stanghellini models is to accurately quantify the surface or internal resistance for vegetable canopies. This study found that there is strong diurnal variation in these resistances to water vapour transport, and therefore they cannot simply be replaced with a constant. The surface and internal resistances depend on the stomatal resistance of the plant, therefore it is recommended to include stomatal resistance measurements in future research.

This study revealed that there are several models using microclimate data around the crop that are able to estimate tomato transpiration in a greenhouse. This indicates that it becomes possible to set the first steps towards predicting future transpiration in further studies. The results show that the following knowledge is missing for the transition towards predictive models. There is a need for stomatal resistance relations with the greenhouse microclimate, it must be known when plants are opening and closing their stomata and thus actively influencing transpiration. Furthermore it is important to study the effect of thermal heating by the plants inside the greenhouse as this study shows that transpiration continues in the evening after the radiation is no longer present. Finally one needs to be able to accurately predict the climate parameters used in the models.

References

- Acquah, S., Yan, H., Zhang, C., Wang, G., Zhao, B., & Wu, H. (2018). Application and evaluation of Stanghellini model in the determination of crop evapotranspiration in a naturally ventilated greenhouse. *International J. Agriculture & Biological Engineering*; 11(6), 95-103.
- Allen, R., Pereira, L., Raes, D., & Smith, M. (1998). *Crop Evapotranspiration; Guidelines for computing crop water requirements*. Rome, Italy: FAO Irrigation and Drainage Paper No. 56.
- Bakker, J. (1991). Leaf conductance of four glasshouse vegetable crops as affected by air humidity. *Agricultural and Forest Meteorology*; 55, 23-36.
- Boulard, T., Roy, J., Pouillard, J., Fatnassi, H., & Grisey, A. (2017). Modelling of micrometeorology, canopy transpiration and photosynthesis in a closed greenhouse using computational fluid dynamics. *Biosystems Engineering*; 158, 110-133.
- CBS. (2022, March 31). *Groenteteelt; oogst en teeltoppervlakte per groentesoort*. Retrieved from Website Centraal Bureau Statistiek: <https://www.cbs.nl/nl-nl/cijfers/detail/37738>
- De Bruin, H., & Stricker, J. (2000). Evaporation of grass under non-restricted soil moisture conditions. *Hydrological Sciences Journal* 45, 391-408.
- Debnath, S., Adamala, S., & Raghuvanshi, N. (2015). Sensitivity Analysis of FAO-56 Penman-Monteith Method for Different Agro-ecological Regions of India. *Environmental Processes*, (2), 689-704.
- Donatelli, M., Bellocchi, G., & Carlini, L. (2006). Sharing knowledge via software components: Models on reference evapotranspiration. *European Journal Agronomy* 24, 186-192.
- Eurostat. (2019, August). *The fruit and vegetable sector in the EU*. Retrieved from Eurostat statistics explained: https://ec.europa.eu/eurostat/statistics-explained/index.php?title=The_fruit_and_vegetable_sector_in_the_EU_-_a_statistical_overview
- Gong, X., Liu, H., Sun, J., Gao, Y., & Zhang, X. (2017). A proposed surface resistance model for the Penman-Monteith formula to estimate evapotranspiration in a solar greenhouse. *Journal Arid Land*, 4, 530-546.
- Gong, X., Wang, S., Xu, C., Zhang, H., & Ze, J. (2020). Evaluation of Several Reference Evapotranspiration Models and Determination of Crop Water Requirement for Tomato in a Solar Greenhouse. *Horticulture Science*; 55(2), 244-250.
- Incrocci, L., Thompson, R., Dolores Fernandez-Fernandez, M., De Pascale, S., Pardossi, A., Stanghellini, C., . . . Gallardo, M. (2020). Irrigation management of European greenhouse vegetable crops. *Agricultural Water Management*, 242, 63-93.
- Karaca, C., Tezcan, A., Büyüktas, D., & Bastug, R. (2018). Equations developed to estimate evapotranspiration in greenhouses. *YYU J Agricultural Science*, 28, (4), 482-489.
- Katsoulas, N., & Stanghellini, C. (2019). Modelling Crop Transpiration in Greenhouses: Different Models for Different Applications. *Agronomy*, 392-409.
- Kim, T., Lee, G., & Youn, B. (2019). Uncertainty characterization under measurement errors using maximum likelihood estimation: cantilever beam end-to-end UQ test problem. *Structural and Multidisciplinary Optimization*, 59, 323-333.

- Miralles, D., Brutsaert, W., Dolman, A., & Gash, J. (2020). On the use of the term "Evapotranspiration". *Water Resources Research* 56, (11).
- Moene, A., & van Dam, J. (2014). *Transport in the Atmosphere-Vegetation-Soil Continuum*. Cambridge, United Kingdom: Cambridge University Press.
- Morile, B., Migeon, C., & Bournet, P. (2013). Is Penman-Monteith model adapted to predict crop transpiration under greenhouse conditions? Application to a New Guinea Impatiens crop. *Scientia Horticulturae*, 152, 80-91.
- Pamungkas, A., Hatou, K., & Morimoto, T. (2014). Evapotranspiration model analysis of crop water use in plant factory system. *Environmental Control in Biology*, 52(3), 183-188.
- Pereira, L., Allen, R., Smith, M., & Raes, D. (2015). Crop evapotranspiration estimation with FAO56: Past and future. *Agricultural Water Management*, 147, 4-20.
- Priestley, C., & Taylor, R. (1972). On the assessment of surface heat flux and evaporation using large-scale parameters. *Monthly Weather Review* 100, (2), 81-92.
- Rakhmanin, V., & Dreyer, H. (2017). *Preface. Good Agricultural Practices for greenhouse vegetable production in the South East European countries. Principles for sustainable intensification of smallholder farms*. Rome, Italy: FAO plant production and protection paper 230; Baudoin, W., Nersisyan, A., Shamilov, A., Hodder, A., Gutierrez, D., De Pascale, S., Nicola, S., Gruda, N., Urban, L., Tany, J.
- Stanghellini, C. (1987). Transpiration of greenhouse crops; an aid to climate management. *Ph.D. Dissertation, Institute of Agricultural Engineering Wageningen, The Netherlands*.
- Stanghellini, C., van 't Ooster, B., & Heuvelink, E. (2019). *Greenhouse Horticulture; Technology for optimal crop production*. Wageningen: Wageningen Academic Publishers.
- Tabari, H., & Talaei, P. (2014). Sensitivity of Evapotranspiration to climatic change in different climates. *Global and Planetary Change*, 115: 16-23.
- Takakura, T., Kubota, C., Sase, S., Hayashi, M., Ishii, M., Takayama, K., . . . Giacomelli, G. (2009). Measurement of evapotranspiration rate in a single-span greenhouse using energy-balance equation. *Biosystems Engineering* 102, (3), 298-304.
- Thompson, R., Incrocci, L., Ruijven, J., & Massa, D. (2020). Reducing contamination of water bodies from European vegetable production systems. *Agricultural Water Management*, 240, 106-111.
- Villarreal-Guerrero, F., Kacira, M., Fitz-Rodríguez, E., Kubota, C., Giacomelli, G., Linker, R., & Arbel, A. (2012). Comparison of three evapotranspiration models for a greenhouse cooling strategy with natural ventilation and variable high pressure fogging. *Scientia Horticulturae*, 210-221.
- Widmoser, P. (2009). A discussion on an alternative fo the Penman-Monteith equation. *Agricultural Water Management*, 96 (4), 711-721.
- Yan, H., Huang, S., Zhang, C., Coenders, M., Wang, G., Zhang, J., . . . Fu, H. (2020). Parameterization and Application of Stanghellini Model for Estimating Greenhouse Cucumber Transpiration. *Water*, 12, 1-14.

Zotarelli, L., Dukes, M., Consuelo, C., Migliaccio, K., & Morgan, K. (2020). Step by step calculation of the Penman-Monteith Evapotranspiration (FAO-56 Method). *Agricultural and Biological Engineering Department, UF/IFAS Extension*, 1-10.

Annex A: Abbreviations

Symbol or abbreviation

C_p	Specific heat of air [$J\ kg^{-1}\ ^\circ C^{-1}$]
G	Soil heat flux density [$W\ m^{-2}$]
h	Coefficient of the convective heat transfer [$W\ m^{-2}\ ^\circ C^{-1}$]
e_a	Actual vapour pressure [Pa]
e_s	Saturation vapour pressure [Pa]
LAI	Leaf area index [$m^2\ m^{-2}$]
LE	Reference evaporation [$W\ m^{-2}$]
Q	Water flux [L^3h^{-1}]
r_a^p	Aerodynamic resistance Penman-Monteith [$s\ m^{-1}$]
r_a^s	Aerodynamic resistance Stanghellini [$s\ m^{-1}$]
r_i	Internal resistance [$s\ m^{-1}$]
r_r	Radiative resistance [$s\ m^{-1}$]
r_s	Surface resistance [$s\ m^{-1}$]
R_n	Net radiation at the crop surface [$W\ m^{-2}$]
S	Water storage [L^3]
T	Air temperature [$^\circ C$]
T_w	Leaf surface temperature [$^\circ C$]
u	Wind speed [ms^{-1}]
α	Dimensionless constant (1.26)
Δ	Slope vapour pressure curve [$Pa\ ^\circ C^{-1}$]
ρ_a	Mean atmospheric density at constant pressure [$kg\ m^{-3}$]
σ	Stefan Boltzmann constant [$J\ m^{-2}\ K^{-4}\ s^{-1}$]
γ	Psychrometric constant [$Pa\ ^\circ C^{-1}$]

Annex B: Pictures Inside Greenhouse

